

tion that younger and weaker Indian crust subducted during the earliest stages of collision would be reflected in a narrower and deeper basin. This early basin subsided rapidly, with sedimentation rates (calculated from the intercalated marl bands)⁵ up to an order of magnitude higher than during later stages of basin evolution in the Neogene¹². Our documentation of the structure of the Balakot Formation not only substantially decreases its stratigraphic thickness, and hence estimates of the depth of the basin at this time, but also shows that the marl bands cannot be used to determine sedimentation rates of the clastic deposits and therefore that there is no constraint on the early sedimentation and subsidence history of the basin. Our new age for the Balakot Formation negates its use as evidence of early orogenic loading and flexural subsidence, and removes the Hazara–Kashmir syntaxis region from its previously anomalous status to the otherwise basin-wide^{13,23} occurrence of a >20 Myr unconformity separating marine and continental facies. □

Received 6 April; accepted 11 December 2000.

1. Ruddiman, W. F. & Kutzbach, J. E. Plateau uplift and climate change. *Sci. Am.* **264**, 42–50 (1991).
2. Krishnaswami, S., Trivedi, J. R., Sarin, M., Ramesh, R. & Sharma, K. Strontium isotopes and rubidium in the Ganga–Bramaputra rivers system: Weathering in the Himalaya, fluxes to the Bay of Bengal and contributions to the evolution of oceanic ⁸⁷Sr/⁸⁶Sr. *Earth Planet. Sci. Lett.* **109**, 2443–253 (1992).
3. Richter, F. M., Rowley, D. B. & DePaolo, D. J. Sr isotopic evolution of seawater: the role of tectonics. *Earth Planet. Sci. Lett.* **109**, 11–23 (1992).
4. Houseman, G. & England, P. Crustal thickening versus lateral expulsion in the Indian–Asian continental collision. *J. Geophys. Res.* **98**, 12233–12249 (1993).
5. Bossart, P. & Ottiger, R. Rocks of the Murree Formation in Northern Pakistan: indicators of a descending foreland basin of late Palaeocene to middle Eocene age. *Ecol. Geol. Helv.* **82**, 133–165 (1989).
6. Rowley, D. B. Age of initiation of collision between India and Eurasia: A review of stratigraphic data. *Earth Planet. Sci. Lett.* **145**, 1–13 (1996).
7. Rowley, D. B. Minimum age of initiation of collision between India and Eurasia north of Everest based on the subsidence history of the Zhepure mountain section. *J. Geol.* **106**, 229–235 (1998).
8. Uddin, A. & Lundberg, N. Cenozoic history of the Himalayan–Bengal system: Sand composition in the Bengal Basin, Bangladesh. *Geol. Soc. Am. Bull.* **110**, 497–511 (1998).
9. Treloar, P. J., Rex, D. C. & Williams, M. P. The role of erosion and extension in unroofing the Indian Plate thrust stack, Pakistan Himalaya. *Geol. Mag.* **128**, 465–478 (1991).
10. Treloar, P. J. Exhumation of high-grade Indian Plate rocks in North Pakistan: Mechanical implications of a multi-phase process. *Terra Nostra* **2**, 157–158 (1999).
11. Critelli, S. & Garzanti, E. Provenance of the Lower Tertiary Murree redbeds (Hazara–Kashmir Syntaxis, Pakistan) and initial rising of the Himalayas. *Sedim. Geol.* **89**, 265–284 (1994).
12. Burbank, D. W., Beck, R. A. & Mulder, T. The Himalayan foreland basin. In *The Tectonic Evolution of Asia* (eds Yin, A. & Harrison, T. M.) 149–188 (Cambridge Univ. Press, 1996).
13. Najman, Y. M. R., Pringle, M. S., Johnson, M. R. W., Robertson, A. H. F. & Wijbrans, J. R. Laser ⁴⁰Ar/³⁹Ar dating of single detrital muscovite grains from early foreland basin sediments in India: Implications for early Himalayan evolution. *Geology* **25**, 535–538 (1997).
14. Pivnik, D. A. & Wells, N. A. The transition from Tethys to the Himalaya as recorded in northwest Pakistan. *Geol. Soc. Am. Bull.* **108**, 1295–1313 (1996).
15. Clauer, N. & Chaudri, S. Isotopic dating of very low-grade metasedimentary and metavolcanic rocks: techniques and methods. In *Low Grade Metamorphism* (eds Frey, M. & Robinson, D.) 202–226 (Blackwell Science, 1999).
16. Bossart, P. *Eine Neuinterpretation der Tektonik der Hazara Kashmir Syntaxis (Pakistan)*. Thesis, ETH Zurich, Switzerland (1986).
17. Kubler, B. La cristallinité de l'illite à les zones tout a fait supérieures du métamorphisme. In *Étages Tectoniques* 105–122. (A la Baconnière, Neuchâtel, Switzerland, 1967).
18. Blenkinsop, T. G. Definition of low-grade metamorphic zones using illite crystallinity. *J. Met. Petrol.* **6**, 623–636 (1988).
19. Weber, K. Notes on the determination of illite crystallinity. *Neues Jb. Miner. Monatshefte* **6**, 267–276 (1972).
20. Butler, R. When did India hit Asia? *Nature* **373**, 20–21 (1995).
21. Garzanti, E., Baud, A. & Mascle, G. Sedimentary record of the northward flight of India and its collision with Eurasia (Ladakh Himalaya, India). *Geodinim. Acta* **1**, 297–312 (1987).
22. Garzanti, E., Critelli, S. & Ingersoll, R. V. Paleogeographic and paleotectonic evolution of the Himalayan range as reflected by detrital modes of Tertiary sandstones and modern sands (Indus transects, India and Pakistan). *Geol. Soc. Am. Bull.* **108**, 631–642 (1996).
23. DeCelles, P. G., Gehrels, G. E., Quade, J. & Ojha, T. P. Eocene–early Miocene foreland basin development and the history of Himalayan thrusting, western and central Nepal. *Tectonics* **17**, 741–765 (1998).
24. Richards, J. P., Noble, S. R. & Pringle, M. S. A revised Late Eocene age for porphyry Cu magmatism in the Escondida Area, Northern Chile. *Econ. Geol.* **94**, 1231–1248 (1999).

Supplementary information is available on Nature's World-Wide Web site (<http://www.nature.com>) or as paper copy from the London editorial office of Nature.

Acknowledgements

We thank E. Laws for field assistance, I. Hussain and Banares for driving, and Major Saeed for his co-operation during major road building; R. Marr, J. Nicholls and M. Stout for

assistance with the electron probe analyses; B. Davidson and J. Imlach for assistance with the Ar–Ar analyses; A. Calder for performing the illite crystallinity analyses; N. Portelance for drafting some of the figures; and D. Burbank and P. Copeland for critical reviews. This work was funded by a Royal Society Dorothy Hodgkin Fellowship and completed during a Royal Society International Fellowship to Y.N. Additional support was provided by the Fold–Fault Research Project at the University of Calgary and a Royal Society Research Grant to Y.N. Ar–Ar analyses were funded by NERC support of the Argon Isotope Facility at the Scottish Universities Environmental Research Centre (SUERC).

Correspondence and requests for materials should be addressed to Y.N. (e-mail: y.najman@glg.ed.ac.uk).

.....
Evidence for mantle metasomatism by hydrous silicic melts derived from subducted oceanic crust

Gaëlle Prouteau*†, Bruno Scaillet‡, Michel Pichavant‡ & René Maury*

* UMR 6538, UBO, 6 avenue Le Gorgeu, P.B. 809, 29285 Brest, France

‡ UMR G113, ISTO, 1a rue de la Férollerie, 45071 Orléans, France

.....
 The low concentrations of niobium, tantalum and titanium observed in island-arc basalts are thought to result from modification of the sub-arc mantle by a metasomatic agent, deficient in these elements, that originates from within the subducted oceanic crust¹. Whether this agent is an hydrous fluid² or a silica-rich melt³ has been discussed using mainly a trace-element approach⁴ and related to variable thermal regimes of subduction zones⁵. Melting of basalt in the absence of fluid both requires high temperatures and yields melt compositions unlike those found in most modern or Mesozoic island arcs^{6,7}. Thus, metasomatism by fluids has been thought to be the most common situation. Here, however, we show that the melting of basalt under both H₂O-added and low-temperature conditions can yield extremely alkali-rich silicic liquids, the alkali content of which increases with pressure. These liquids are deficient in titanium and in the elements niobium and tantalum and are virtually identical to glasses preserved in mantle xenoliths found in subduction zones⁶ and to veins found in exhumed metamorphic terranes of fossil convergent zones⁷. We also found that the interaction between such liquids and mantle olivine produces modal mineralogies that are identical to those observed in metasomatized Alpine-type peridotites⁸. We therefore suggest that mantle metasomatism by slab-derived melt is a more common process than previously thought.

A mid-ocean ridge basalt from the Juan de Fuca ridge (Table 1) was reacted between 10 and 30 kbar with bulk H₂O contents of 2 to 10 wt% (see ref. 9 for methods), that is, largely in excess of the H₂O content of metamorphosed basalts, and at temperatures below 1,000 °C. Recent experimental work has shown that melting under these conditions (addition of H₂O, low temperatures) is required to account for the geochemical and physical characteristics of slab melts⁹, and approaches the most likely pressure–temperature (P–T) conditions for slab melting (750 °C, 30 kbar) as constrained from thermal modelling¹⁰.

Representative glass (that is, quench melt) compositions are listed in Table 1. In a An–Ab–Or projection (Fig. 1), the glass compositions define a trend parallel to the albite–anorthite join. Glasses

† Present address: Laboratoire de Pétrologie, UPMC, 4 Place Jussieu, 75252, Paris, France.

produced at both 10 and 20 kbar cluster in the tonalitic field, whereas those obtained at 30 kbar fall within the trondhjemite field. The latter have Na₂O contents in excess of 7 wt%, increasing as temperature decreases, and are clearly peralkaline (molar Al₂O₃/Na₂O+K₂O+CaO<1), whereas all the glasses produced at lower pressures tend to be either metaluminous or slightly peraluminous. The reason for the large compositional jump observed between 10–20 and 30 kbar is that amphibole breaks down in this pressure range, and the modal abundances of garnet and clinopyroxene increase. The Na₂O released by the amphibole breakdown is not fully balanced by the increase in the Na content of clinopyroxene (that is, the jadeite component) and thus, for a given *T* and bulk H₂O content, the liquid becomes more sodic and less calcic as pressure increases beyond the amphibole stability field. Extensive garnet crystallization at 30 kbar also lowers the Al₂O₃ content of the glasses relative to those at 20 kbar (Table 1). In the CaO versus Na₂O diagram (Fig. 2), all glasses so far produced in H₂O-added melting experiments on basalts up to 30 kbar^{11–13} display a broad negative trend that completely overlaps that field of natural glasses or veins believed to be slab melts^{6,7}, in contrast to results from dehydration melting experiments^{13–15} (Fig. 2b). A similar feature is observed for other elements such as FeO or TiO₂. The melt TiO₂ content (Table 1) agrees with existing rutile solubility models¹⁶. At pressures lower

than 10 kbar the glasses are characterized by high CaO and relatively low Na₂O contents, as well as a high Al₂O₃ content, due to the lack of both plagioclase and garnet in the residue^{12,13}. In contrast, glasses obtained in the pressure range 20–30 kbar coexist with an eclogitic residue. Results obtained at 30 kbar match the composition of metasomatic veins the most closely, in particular the extreme Na₂O enrichment. This suggests that these experimental conditions—temperatures below 900 °C and bulk water content around 5–6 wt%, thus requiring the presence of a fluid phase before melting—reproduce those of vein production. The origin of free water may lie in the dehydration of serpentinite beneath the oceanic crust of the subducted plate^{17,18}. The water thus produced is expected to dissolve in the melt, except at low melt fraction where there may be enough water to saturate the melt. Clearly, these conditions of slab melting better approach those predicted from thermal modelling¹⁰ than do the conditions of the dehydration melting experiments. Therefore, we conclude that free water is needed at depth for slab melting to occur in present-day subduction zones. Experimental constraints on slab melts predict meltwater contents of at least 15 wt% (ref. 9), whereas mass balance calculations on the run products obtained at 30 kbar yield meltwater contents between 24 and 30 wt%. The unusual major-element composition of slab melts appears to be more characteristic of their origin than their trace element signature. In particular, melting in the garnet field of basalt underplated beneath the continental crust may yield silicic melts with trace element patterns similar to those of slab melts¹⁹, but they will be granitic instead of trondhjemitic because less water is available in the lower crust and dehydration melting reactions are favoured.

Interaction of such trondhjemitic melts with the overlying mantle wedge has been experimentally simulated at 15 kbar, as in previous similar works^{20–22}, by mixing a synthetic equivalent of the trondhjemite melt obtained during melting of the basalt with a forsteritic olivine (Fo 90), the dominant mineral in peridotites (Table 2). Liquid and mineral compositions are listed in Table 2. At 1,000 °C, an orthopyroxene+liquid assemblage is produced. At 900 °C, in addition to orthopyroxene, both an amphibole and phlogopite are reaction products of the interaction process. At both temperatures, olivine appears not to be stable, although residual crystals persist. Glass compositions are notably more magnesian and silica-poor than the starting trondhjemite, being dacitic instead of rhyolitic, yet their strongly alkali-rich character still persists or even increases (Table 2). An increase of the Mg/(Mg+Fe) ratio of the liquid together with massive orthopyroxene crystallization are key features of geochemical models of slab melt/peridotite interaction²³ and reproduce diagnostic petrographic characteristics of slab-derived magmas²⁴. In addition, the compositions of amphibole and phlogopite, the two main minerals diagnostic of mantle

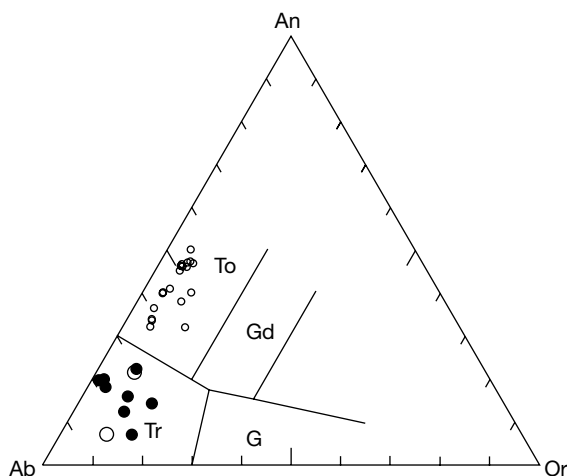


Figure 1 Normative (CIPW) compositions of natural slab melts (black circles) and of glasses obtained in melting experiments of basalts with added H₂O (this study). Small white circles represent experiments done at or below 20 kbar and large white circles experiments at 30 kbar. An, anorthite; Ab, albite; Or, orthoclase; To, tonalite, Tr, trondhjemite; Gd, granodiorite; G, granite.

Table 1 Experimental and natural glass/vein compositions and experimental phase proportions

	<i>P</i> (kbar)	<i>T</i> (°C)	H ₂ O*	SiO ₂	TiO ₂	Al ₂ O ₃	FeO†	MgO	CaO	Na ₂ O	K ₂ O	Gl	Hbl	Cpx	Gt	Tmt	Ilm	Rut	Sph
Experimental glasses from hydrous basalt melting																			
Starting‡	–	–	–	49.9	2.3	13.7	12.7	6.8	10.6	2.5	0.3	–	–	–	–	–	–	–	–
27	10	841	9.9	69.8	0.2	18.7	0.9	0.5	5.8	3.4	0.6	41.1	26.0	21.7	–	8.6	2.6	–	–
38	20	800	9.2	68.8	0.3	16.7	2.9	1.0	5.9	3.4	0.7	28.0	67.4	–	–	–	0.1	–	7.0
39	20	900	10.2	65.4	0.4	20.9	1.7	0.2	7.0	3.7	0.6	36.2	39.1	20.9	–	–	4.0	–	–
40	20	1,000	10.0	59.3	1.5	20.1	5.1	0.9	7.5	4.3	0.8	46.8	26.5	20.8	–	5.9	–	–	–
41	30	900	6.4	70.9	0.3	16.1	0.5	0.1	1.4	9.3	1.5	23.9	–	42.9	31.8	–	0.4	0.9	–
42	30	1,000	6.0	68.0	0.6	17.9	1.2	0.2	3.7	7.1	1.1	25.6	–	34.8	38.4	–	–	1.1	–
Felsic veins in mantle xenoliths or in metamorphic complexes from subduction zones																			
Val55/4	–	–	–	67.8	0.4	18.0	0.6	0.2	1.1	7.9	2.1	–	–	–	–	–	–	–	–
Val55/4	–	–	–	63.9	0.9	19.7	2.7	1.0	3.0	5.7	0.9	–	–	–	–	–	–	–	–
41867A	–	–	–	72.2	0.1	16.5	0.2	0.1	2.8	6.6	0.3	–	–	–	–	–	–	–	–

Analyses and phase proportions given in wt%. Glass analyses normalized to 100% anhydrous. Gl, glass; Hbl, hornblende; Cpx, clinopyroxene; Gt, garnet; Tmt, titanomagnetite; Ilm, ilmenite; Rut, rutile; Sph, sphene. Run durations are between 25 h at 1,000 °C to 144 h at 841 °C, see ref. 9 for methods. Glass compositions Val55/4 are from ref. 6. The pegmatite vein 41867A is from ref. 7.

* H₂O loaded to the capsule.

† Total Fe calculated as FeO.

‡ Dry starting glass composition used in crystallization experiments.

metasomatism, are remarkably similar to those of natural amphibole and phlogopite found in some Alpine-type peridotite complexes believed to have been pervasively metasomatized by infiltrating slab-derived melts⁸. In particular, both minerals are characterized by high Mg/(Fe+Mg) ratios and display strong enrichment in Na₂O. Given the large number of parameters involved in the interaction process (that is, compositions of peridotite and infiltrating melt, solid/melt ratio, pressure and temperature of the interaction) it is expected that metasomatic phases display a wide range of composition, as in previous laboratory studies^{20–22} and natural occurrences²⁵. However, the sodic character of metasomatic minerals can be related to the sodic character of the metasomatizing agent, as evidenced by the trondhjemite veins of Kamchatka. Variable Na₂O enrichment of metasomatic minerals would trace the more or less trondhjemitic character of the percolating melt which in turn depends on the conditions of its genesis, in particular pressure, as shown above. The similarity between the compositions of experimental and natural phases suggests that the interaction experiments reproduce the conditions of mantle metasomatism and in particular the chemistry of the metasomatic agent.

The above experimental evidence bears direct constraints on metasomatic processes in arc settings. The low-temperature, fluid-present melting conditions above suggest that slab melting can occur in presently subducting plates, as previously suggested on geochemical grounds⁵. Although slab melting was originally supposed to have occurred mostly during the Archaean²⁶ or only when young and hot plate subducts in modern settings⁵, the increasing number of occurrences of magmas with slab melt signatures worldwide²⁷ suggests that conditions for slab melting are realized more often than currently believed. The slab melt contribution as a metasomatizing agent of the sub-arc mantle may thus be important. Mass balance calculations indicate that 15 g of trondhjemite yields 1 g of phlogopite upon reaction with peridotite, whereas 180 g of hydrous fluid are needed to precipitate an equivalent mass of phlogopite during a peridotite–fluid interaction²⁸. Thus, as far as metasomatic mineral production is concerned, slab-derived melts are about ten times more efficient than hydrous fluids. Consequently, the geochemical imprint of slab melts can be important in modern arc settings even if slab melting is probably less common than slab dehydration²⁹. In particular, calculated trace-element concentrations in slab melts in equilibrium with an eclogitic residue (garnet+clinopyroxene+/-rutile) are enriched in light-rare-earth and large-ion-lithophile elements and depleted in high-field-strength elements (La/Nb = 7; Ba/Nb = 186; ref. 22) and will

impart their geochemical signature to magmas generated in the mantle wedge²⁴.

The overall slab contribution to the source of arc magmas is estimated not to exceed 3% on the basis of oxygen isotope systematics of oceanic arc lavas³⁰. The reason why slab melts (adakites) are found in volumetrically minor amounts relative to regular calc-alkaline arc magmas may be either physical or chemical. Silica-rich liquids can equilibrate with mantle minerals provided

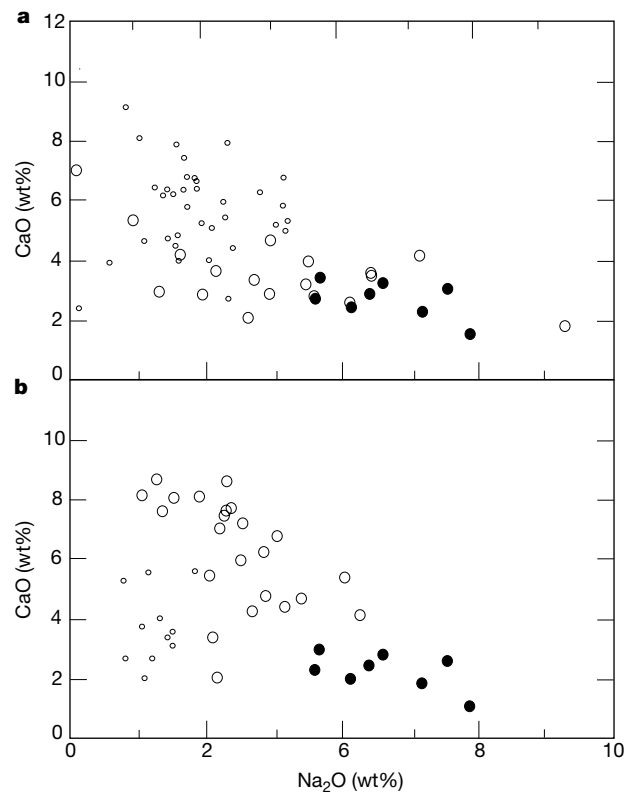


Figure 2 Na₂O versus CaO plot of natural slab melts^{6,7} (black circles) and of glasses obtained in melting experiments (large white circles) using N-MORB type basalt protoliths. **a**, Glasses obtained in melting experiments with added H₂O (this study and refs 11–13). **b**, Glasses obtained in dehydration melting experiments^{13–15}. Small white circles represent experiments done at or below 10 kbar (in both **a** and **b**).

Table 2 Glass and mineral compositions from trondhjemite–Fo90 olivine interactions at 15 kbar

	SiO ₂	TiO ₂	Al ₂ O ₃	FeO*	MgO	CaO	Na ₂ O	K ₂ O	NiO	total
Starting end members										
Trondh	71.2	0.5	16.9	0.5	0.1	1.5	7.8	1.5	–	100
Olivine	40.8	–	0.1	10.8	47.8	–	–	–	0.3	99.7
Run product compositions										
1,000 °C, 7.8 wt% H ₂ O†										
Gl	65.9	0.5	17.6	1.0	2.9	1.4	8.9	1.6	<0.1	92.2
Opx	58.3	0.1	0.8	3.8	35.3	0.9	0.1	–	0.2	99.5
900 °C, 9.6 wt% H ₂ O										
Gl	64.2	0.5	18.8	1.1	1.5	1.0	11.4	1.5	<0.1	89.6
Opx	57.7	0.1	0.8	6.0	33.4	0.9	0.2	–	0.2	99.4
Phl	41.9	1.6	14.2	2.9	24.4	–	2.7	6.3	0.2	94.4
Amph	50.9	1.7	6.1	3.5	20.6	8.9	4.2	0.3	0.1	96.5
Hydrous phases in metasomatised peridotite‡										
Phl	41.9	0.7	14.3	2.8	25.3	0.0	1.6	6.5	–	94.6
Amph	49.9	0.4	7.5	3.4	20.2	10.2	3.8	0.6	–	98.3

Mixtures consisted in 60 wt% trondhjemite dry glass and 40 wt% olivine. Analyses given in wt%. Glass analyses normalized to 100% anhydrous. Gl, glass; Opx, orthopyroxene; Phl, phlogopite; Amph, amphibole; trondh, trondhjemite.

* Total Fe calculated as FeO.

† Bulk H₂O content of the charge and temperature of the interaction experiment.

‡ Phlogopite and amphibole from the Finero peridotite massif⁸.

they are alkali-rich³¹. This alkali effect is most pronounced at pressures below 20 kbar, however. At 30 kbar, liquids in equilibrium with mantle peridotite are not alkali-rich. The alkali content of experimental slab melts increases with pressure, and comparison with their natural equivalents has shown that slab melting is likely to occur at 30 kbar or more. Thus, besides the physical aspects of magma transport and percolation, any alkali-rich slab melt produced at or beyond 30 kbar, as in our experiments, will be in strong chemical disequilibrium with the overlying mantle wedge. Extensive interaction between these melts and peridotite is expected to occur and the alkali-rich, silica-rich melts will have little opportunity to reach shallower levels unchanged. On this basis, preservation or eruption of genuine slab melts can be anticipated to be difficult, accounting for their relative rarity in most arcs. The chemical differences observed between experimentally produced slab-melts and those erupted or preserved as melt inclusions³² must in fact reflect various extents of interaction of the latter with mantle material during upward migration. □

Received 22 June 2000; accepted 16 January 2001.

- Hofmann, A. W. Chemical differentiation of the Earth: the relationships between mantle, continental crust, and oceanic crust. *Earth Planet. Sci. Lett.* **90**, 297–314 (1988).
- Eiler, J. M., McInnes, B., Valley, J. W., Graham, C. M. & Stolper, E. M. Oxygen isotope evidence for slab-derived fluids in the sub-arc mantle. *Nature* **393**, 777–781 (1998).
- Nicholls, I. A. & Ringwood, A. E. Effect of water on olivine stability in tholeiites and production of silica saturated magmas in island arc environment. *J. Geol.* **81**, 285–300 (1973).
- Hawkesworth, C. J., Turner, S. P., McDermott, F., Peate, D. W. & van Calsteren, P. U–Th isotopes in arc magmas: implications for element transfer from the subducted crust. *Science* **276**, 551–555 (1997).
- Defant, M. J. & Drummond, M. S. Derivation of some modern arc magmas by melting of young subducted lithosphere. *Nature* **347**, 662–665 (1990).
- Kepezhinskas, P. K., Defant, M. J. & Drummond, M. S. Na metasomatism in the island-arc mantle by slab melt-peridotite interaction: evidence from mantle xenoliths in the north Kamchatka arc. *J. Petrol.* **36**, 1505–1527 (1995).
- Sorensen, S. S. & Grossman, J. N. Enrichment of trace elements in garnet amphibolites from a paleo-subduction zone: Catalina Schist, southern California. *Geochim. Cosmochim. Acta* **53**, 3155–3177 (1989).
- Zanetti, A., Mazzucchelli, Rivalenti, G. & Vannucci, R. The Finero phlogopite-peridotite massif: an example of subduction-related metasomatism. *Contrib. Mineral. Petrol.* **134**, 107–122 (1999).
- Prouteau, G., Scaillet, B., Pichavant, M. & Maury, R. C. Fluid-present melting of ocean crust in subduction zones. *Geology* **27**, 1111–1114 (1999).
- Peacock, S. M., Rushmer, T. & Thompson, A. B. Partial melting of subducting oceanic crust. *Earth Planet. Sci. Lett.* **121**, 227–244 (1994).
- Whinter, K. T. & Newton, R. C. Experimental melting of hydrous low-K tholeiite: evidence on the origin of Archean cratons. *Bull. Geol. Soc. Denmark* **39**, 213–228 (1991).
- Spulber, S. D. & Rutherford, M. J. The origin of rhyolite and plagiogranite in oceanic crust: an experimental study. *J. Petrol.* **24**, 1–25 (1983).
- Beard, J. S. & Lofgren, G. E. Dehydration melting and water-saturated melting of basaltic and andesitic greenstones and amphibolites at 1, 3, and 6.9 kb. *J. Petrol.* **32**, 365–401 (1991).
- Rapp, R. P. & Watson, E. B. Dehydration melting of metabasalt at 8–32 kbar: implications for continental growth and crust-mantle recycling. *J. Petrol.* **36**, 891–931 (1995).
- Sen, C. & Dunn, T. Dehydration melting of a basaltic composition amphibolite at 1.5 and 2.0 GPa: implications for the origin of adakites. *Contrib. Mineral. Petrol.* **117**, 394–409 (1994).
- Ryerson, F. J. & Watson, E. B. Rutile saturation in magmas: implications for Ti-Nb-Ta depletion in island-arc basalts. *Earth Planet. Sci. Lett.* **86**, 225–239 (1987).
- Ulmer, P. & Trommsdorff, V. Serpentine stability to mantle depths and subduction-related magmatism. *Science* **268**, 858–861 (1995).
- Schmidt, M. & Poli, S. Experimentally based water budget for dehydrating slabs and consequences for arc magma generation. *Earth Planet. Sci. Lett.* **163**, 361–379 (1998).
- Atherton, M. P. & Petford, N. Generation of sodium-rich magmas from newly underplated basaltic crust. *Nature* **362**, 144–146 (1993).
- Carroll, M. J. & Wyllie, P. J. Experimental phase relations in the system peridotite-tonalite-H₂O at 15 kbar: implications for assimilation and differentiation processes at the crust-mantle boundary. *J. Petrol.* **30**, 1351–1382 (1989).
- Sen, C. & Dunn, T. Experimental modal metasomatism of a spinel lherzolite and the production of amphibole-bearing peridotite. *Contrib. Mineral. Petrol.* **119**, 422–432 (1994).
- Rapp, R. P., Shimizu, N., Norman, M. D. & Applegate, G. S. Reaction between slab-derived melts and peridotite in the mantle wedge: experimental constraints at 3.8 GPa. *Chem. Geol.* **160**, 335–356 (1999).
- Kelemen, P., Shimizu, N. & Dunn, T. Relative depletion of niobium in some arc magmas and the continental crust: partitioning of K, Nb, La, and Ce during melt/rock reaction in the upper mantle. *Earth Planet. Sci. Lett.* **120**, 111–134 (1993).
- Yogodzinski, G. M., Volynets, O. N., Koloskov, A. V. & Seliverstov, N. I. Magnesian andesites and the subduction component in a strongly calcalkaline series at Piip volcano, far western Aleutian. *J. Petrol.* **34**, 163–204 (1994).
- Ionov, D. A. & Hofmann, A. W. Nb-Ta-rich mantle amphiboles and micas: implications for subduction-related metasomatic trace element fractionations. *Chem. Geol.* **131**, 341–356 (1995).
- Martin, H. Effect of steeper Archean geothermal gradient on geochemistry of subduction zone magmas. *Geology* **14**, 753–756 (1986).
- Drummond, M. S., Defant, M. J. & Kepezhinskas, P. K. Petrogenesis of slab derived-tonalite-dacite adakite magmas. *Trans. R. Soc. Edinburgh* **87**, 205–215 (1996).

- Schneider, M. E. & Eggler, D. H. Fluids in equilibrium with peridotite minerals: implications for mantle metasomatism. *Geochim. Cosmochim. Acta* **50**, 711–724 (1986).
- Tatsumi, Y. Migration of fluid phases and genesis of basalt magmas in subduction zones. *J. Geophys. Res.* **94**, 4697–4707 (1989).
- Eiler, J. M. *et al.* Oxygen isotopes geochemistry of oceanic-arc lavas. *J. Petrol.* **41**, 229–256 (2000).
- Hirschman, M. M., Baker, M. B. & Stolper, E. M. The effect of alkalis on the silica content of mantle-derived melts. *Geochim. Cosmochim. Acta* **62**, 883–902 (1998).
- Schiano, P. *et al.* Hydrous, silica-rich melts in the sub-arc mantle and their relationship with erupted arc-lavas. *Nature* **377**, 595–600 (1995).

Correspondence and requests for materials should be addressed to B.S. (e-mail: bscaille@cnsr-orleans.fr).

Branched integumental structures in *Sinornithosaurus* and the origin of feathers

Xing Xu*, Zhong-he Zhou* & Richard O. Prum†

* Institute of Vertebrate Paleontology and Paleoanthropology, Academia Sinica, PO Box 643, Beijing, 100044, People's Republic of China

† Department of Ecology and Evolutionary Biology, and Natural History Museum, University of Kansas, Lawrence, Kansas 66045, USA

The evolutionary origin of feathers has long been obscured because no morphological antecedents were known to the earliest, structurally modern feathers of *Archaeopteryx*¹. It has been proposed that the filamentous integumental appendages on several theropod dinosaurs are primitive feathers^{2–6}; but the homology between these filamentous structures and feathers has been disputed^{7–9}, and two taxa with true feathers (*Caudipteryx* and *Protarchaeopteryx*) have been proposed to be flightless birds^{8,10}. Confirmation of the theropod origin of feathers requires documentation of unambiguously feather-like structures in a clearly non-avian theropod. Here we describe our observations of the filamentous integumental appendages of the basal dromaeosaurid dinosaur *Sinornithosaurus millenii*, which indicate that they are compound structures composed of multiple filaments. Furthermore, these appendages exhibit two types of branching structure that are unique to avian feathers: filaments joined in a basal tuft, and filaments joined at their bases in series along a central filament. Combined with the independent phylogenetic evidence supporting the theropod ancestry of birds^{11–13}, these observations strongly corroborate the hypothesis that the integumental appendages of *Sinornithosaurus* are homologous with avian feathers. The plesiomorphic feathers of *Sinornithosaurus* also conform to the predictions of an independent, developmental model of the evolutionary origin of feathers¹⁴.

Sinornithosaurus millenii (Fig. 1) is a non-avian, basal dromaeosaurid dinosaur from the Lower Cretaceous Yixian formation (~124.6 Myr ago), Liaoning, China⁵. Along with *Sinosauropteryx*³ (a basal coelurosaur), *Beipiaosaurus*⁴ (a therizinosauroid) and *Microraptor*⁶ (a dromeosaur), *Sinornithosaurus*⁵ has many filamentous integumental structures that may be plesiomorphic feathers. As in *Beipiaosaurus* and *Microraptor*, the filamentous integumental appendages of *Sinornithosaurus* are indistinguishable from the contour feathers of birds preserved in the same deposits (compared with holotypes of *Confuciusornis sanctus*, *Eoenantiornis buhler* and *Chanchengornis hengdaoziensis*). In these avian specimens, the indisputable contour feathers on the body are preserved as diffuse arrays of filaments of varying diameters without a prominent rachis or central shaft. Despite these similarities, homology between the